NEUROIMAGE **6,** 104–112 (1997)
ARTICLE NO. NI970282

Quantitation of Regional Cerebral Blood Flow Increases during Motor Activation: A Steady-State Arterial Spin Tagging Study

Frank Q. Ye,* Anne M. Smith,† Yihong Yang,† Jeff Duyn,† Venkata S. Mattay,* Urs E. Ruttimann,‡ Joseph A. Frank,† Daniel R. Weinberger,* and Alan C. McLaughlin*

**Clinical Brain Disorders Branch, NIMH, †Laboratory of Diagnostic Radiology Research, OIR, and ‡Laboratory of Clinical Studies, NIAAA, National Institutes of Health, Bethesda, Maryland 20892*

Received March 24, 1997

Steady-state arterial spin tagging MRI approaches were used to quantitate regional cerebral blood flow increases during finger tapping tasks in seven normal subjects. Statistically significant increases in cerebral blood flow were observed in the contralateral primary sensorimotor cortex in all seven subjects and in the supplementary motor area in five subjects. The intrinsic spatial resolution of the cerebral blood flow images was ~4 mm. If no spatial filtering was applied, the average increase in cerebral blood flow in the activated primary sensorimotor cortex was 60 ± 10 cc/100 g/min (91 ± 32%). If the images were filtered to a spatial resolution of 15 mm, the average increase in cerebral blood flow in the activated primary sensorimotor cortex was 23 ± 7 cc/100 g/min (42 ± 15%), in agreement with previously reported ^{133}Xe and PET results. © 1997 Academic Press

INTRODUCTION

BOLD MRI approaches (Kwong *et al.,* 1992; Ogawa *et al.,* 1992; Bandettini *et al.,* 1992) have been used for a number of years to image regional cerebral "activation" during visual, motor, and cognitive tasks. Dynamic arterial spin tagging MRI approaches such as EPISTAR (Edelman *et al.,* 1994) and FAIR (Kwong *et al.,* 1995; Kim *et al.,* 1995; Kim and Tsekos, 1997) have recently been used for the same purpose.

Steady-state arterial spin tagging MRI approaches (Detre *et al.,* 1992; Williams *et al.,* 1992) can give quantitative images of cerebral blood flow in humans (Roberts *et al.,* 1994; Ye *et al.,* 1996; Alsop and Detre, 1996; Ye *et al.,* 1997a) and have been validated against ^{15}O PET techniques (Ye *et al.,* 1997b). A recent report (Talagala *et al.,* 1996) suggested that steady-state arterial spin tagging approaches could be used to image cerebral blood flow increases during visual stimulation. The aim of the work presented here was to investigate if steady-state arterial spin tagging approaches could provide quantitative images of regional cerebral blood flow increases during motor activation paradigms.

MATERIALS AND METHODS

Experimental Protocol

Experiments were performed on seven normal, right-handed subjects (three males and four females), using a protocol approved by the Institutional Review Board of the National Institute of Mental Health.

A series of axial images were examined to locate the primary sensorimotor cortex. An anatomical MR image of an axial slice including the primary motor cortex was acquired, and spin tagging approaches (see below) were used to acquire 96 perfusion images of the slice over a 30-min period. During this 30-min period subjects alternated between intervals of rest and intervals of finger tapping: both the rest interval and the tapping interval were 150 s long. Finger tapping involved self-paced sequential apposition of the fingers of the right hand against the right thumb at a frequency of ~2 Hz.

MR Imaging

All experiments were performed on a Signa 1.5 T (General Electric, Milwaukee, WI) scanner using a standard quadrature head coil and a standard body-gradient coil capable of a maximum amplitude of 22 mT/m and a maximum slew rate of 120 T/m/s. Anatomical images were acquired using a spin-echo sequence with a 256 × 256 matrix and a slice thickness of 5 mm; TE = 14 ms, TR = 500 ms.

Single-shot 2D spin-echo SPIRAL images (Yang *et al.,* 1996) were obtained using a 64 × 64 matrix, a 24-cm field of view, and a slice thickness of 5 mm; TE = 19 ms, TR = 4.7 s. A fat saturation pulse, consisting of a 16-ms nonselective sinc pulse followed by gradient spoiler pulses, was added to the sequence before the 90° excitation pulse. The total length of the SPIRAL waveform was 22 ms.

1053-8119/97 $25.00
Copyright © 1997 by Academic Press
All rights of reproduction in any form reserved.

Symmetrical gradients (22 mT/m) were placed immediately before and after the 180° pulse to "crush" the signal from arterial water spins: the width of each gradient pulse was 5.6 ms, and the separation between the gradient pulses was 3.6 ms (b = 7.8 s/mm^2). The length and the separation of the gradients were chosen to crush adequately the arterial blood signal, while minimizing nonspecific effects due to gross motion (Ye *et al.*, 1997a).

The T_1 relaxation rate in the absence (R_{10}) and presence ($R_1(\omega_1,\Delta\omega)$) of off-resonance radiofrequency (rf) irradiation were determined for each voxel in the SPIRAL image using procedures described previously (Ye *et al.*, 1997a).

Spin Tagging

Flow-induced adiabatic inversion (Williams *et al.*, 1992) was used to invert arterial water spins flowing through the "tagging" plane, which was placed approximately 3 cm below the center of the imaging slice (Fig. 1). Inversion was accomplished using a 3.5-s off-resonance rf pulse train in the presence of a z gradient. The pulse train consisted of rectangular rf pulses of 75 ms duration separated by 10 ms. The amplitude of the off-resonance rf field (γB_1) was 170 Hz. This value was chosen because previous studies suggested that it produced maximum inversion of arterial water spins at the tagging plane under our conditions (Ye *et al.*, 1996). The frequency off-set of the irradiating rf field (±6000 Hz) and the sign of the z gradient (±4.8 mT/m) were alternated in a four-step protocol to minimize the influence of asymmetric magnetization transfer effects and gradient eddy currents (Pekar *et al.*, 1996). Each perfusion image was calculated using the data collected in a single "four-pulse" protocol (see below). The data collection time for a single four-pulse protocol was 18.8 s.

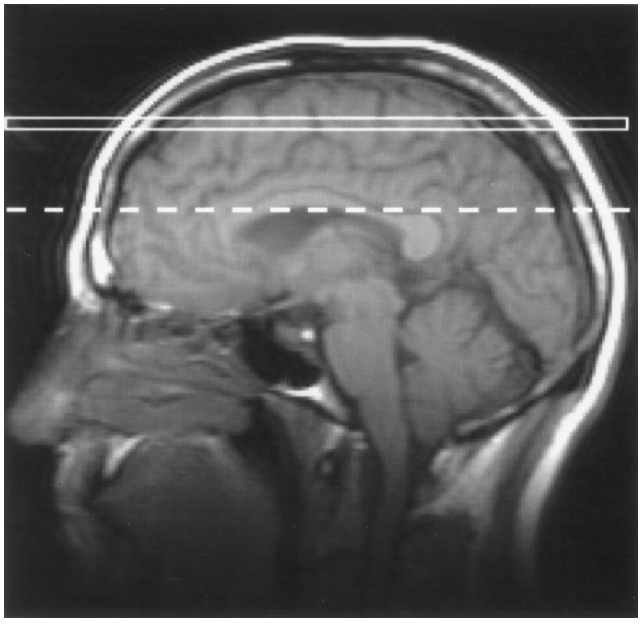

FIG. 1. Sagittal image of a human head, showing the approximate location of the imaging slice (solid lines) and the inversion plane (dashed line) used for the perfusion imaging experiments.

Arterial spin tagging data were acquired using a "delayed acquisition" approach (Alsop and Detre, 1996; Ye *et al.*, 1997c). In this approach a delay, τ_{delay}, was inserted between the end of the tagging period and the beginning of the acquisition of the SPIRAL image. If τ_{delay} is longer than the arterial transit time, τ_a, cerebral blood flow values, Q, can be calculated using the equation (Ye *et al.*, 1997c)

$$\frac{\Delta M(\tau_{delay})}{M_0} = -\frac{2\alpha_0 Q/\lambda}{R_{10}} e^{-R_{10}\tau_{delay}} \{1 - \Psi_1 - \Psi_2\}\{\Psi_3\} \quad (1)$$

where

$$\Psi_1 = \left(1 - \frac{R_{10}}{R_1(\omega_1,\Delta\omega)}\right) e^{-R_{10}\tau_a}, \quad (2)$$

$$\Psi_2 = \frac{R_{10}}{R_1(\omega_1,\Delta\omega)} e^{-[R_{10}-R_1(\omega_1,\Delta\omega)]\tau_a} e^{-R_1(\omega_1,\Delta\omega)\tau_0}, \quad (3)$$

$$\Psi_3 = e^{[R_{10}-R_{1a}]\tau_a}, \quad (4)$$

and $\Delta M(\tau_{delay})$ is the difference in the MR signal amplitude observed in the presence and absence of arterial tagging, M_0 is the equilibrium value of the MR signal amplitude, R_{1a} is the relaxation rate of arterial water protons, τ_0 is the length of the off-resonance rf irradiation, and α_0 is the extent of inversion of arterial water in the tagging plane. R_{1a} was assumed to be 0.8 s^{-1}, τ_a was assumed to be 0.95 s, and α_0 was assumed to be equal to the duty cycle of the rf pulse train, i.e., 0.88 (Ye *et al.*, 1997a). τ_{delay} = 1.1 s and τ_0 = 3.5 s.

Processing of Cerebral Blood Flow Difference Images

The voxel size for the 64 × 64 cerebral blood flow images was 3.75 mm × 3.75 mm. Cerebral blood flow images were interpolated with zeros from 64 × 64 to 256 × 256 and convolved with a two-dimensional Gaussian kernel. The full-width-at-half-maximum (FWHM) of the Gaussian kernel varied from 0 to 22.5 mm.

The first cerebral blood flow image was not included in the analysis because of saturation effects. All of the remaining cerebral blood flow images obtained under "rest" conditions were averaged together, and all of the cerebral blood flow images obtained under "finger-tapping" conditions were averaged together. A cerebral blood flow "difference" image was calculated by subtracting these two average images. The "t" score for each

voxel was calculated using the equation (Ott, 1977)

$$t = \frac{\Delta\mathrm{CBF}}{\sigma\sqrt{(1/N_1) + (1/N_2)}}, \tag{5}$$

where ΔCBF is the average cerebral blood flow difference, N_1 is the number of cerebral blood flow measurements analyzed during rest conditions, N_2 is the number of cerebral blood flow measurements analyzed during finger tapping conditions, and σ is the pooled standard deviation of the cerebral blood flow measurements. Under our conditions, $N_1 = 47$ and $N_2 = 48$. σ is given by the equation (Ott, 1977)

$$\sigma^2 = \frac{(N_1 - 1)\sigma_1^2 + (N_2 - 1)\sigma_2^2}{N_1 + N_2 - 2}, \tag{6}$$

where σ_1 is the voxel standard deviation of cerebral blood flow values measured during rest, and σ_2 is the voxel standard deviation of cerebral blood flow values measured during finger tapping.

The number of degrees of freedom of the t field was

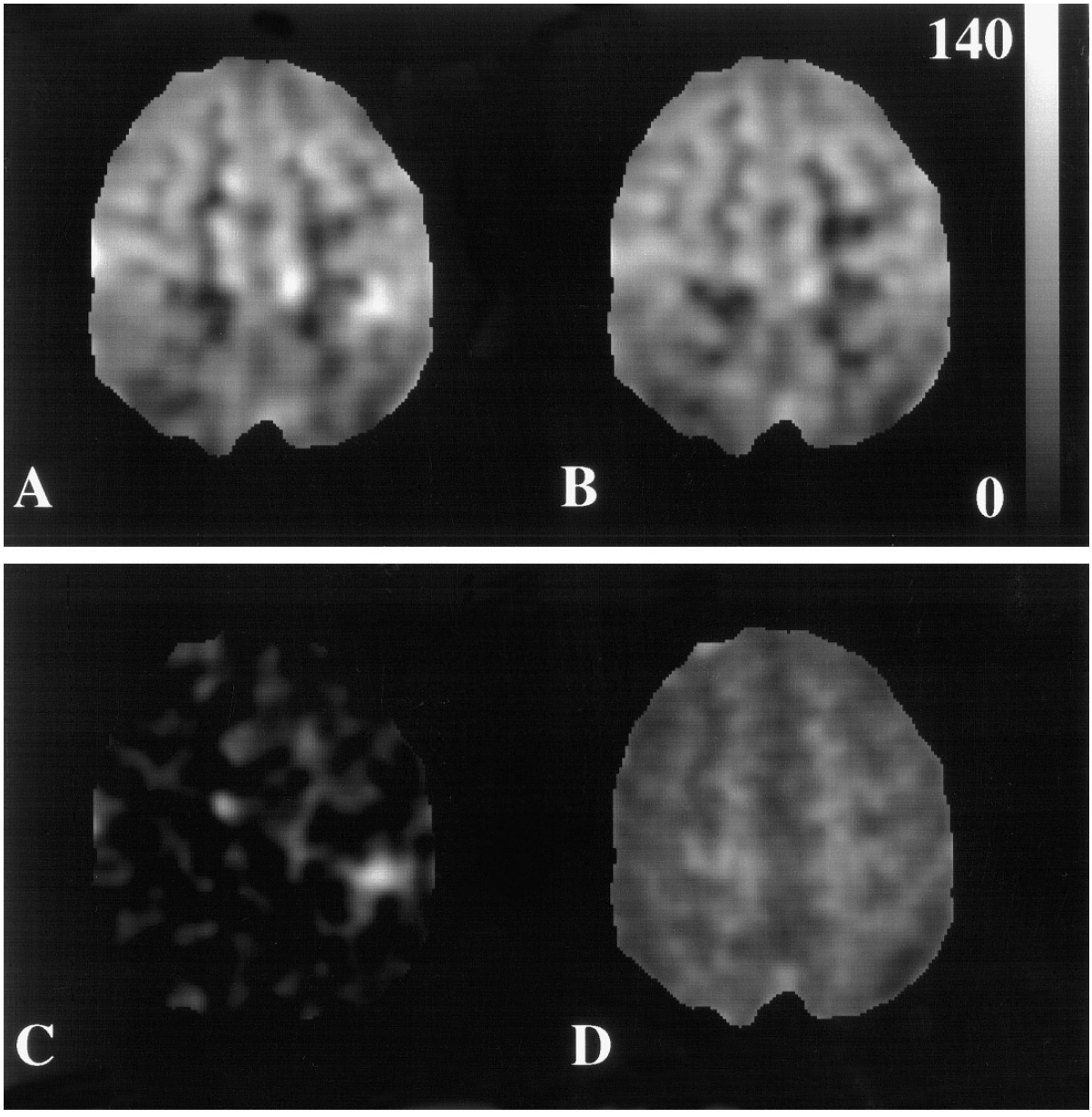

FIG. 2. (A) Cerebral blood flow image of the axial imaging slice (see Fig. 1) during finger tapping; (B) cerebral blood flow image of the same slice during rest; (C) cerebral blood flow difference image; (D) pooled standard deviation map of the cerebral blood flow difference image. Cerebral blood flow images were convolved with a Gaussian kernel having a FWHM of 5.6 mm. Data from subject 3.

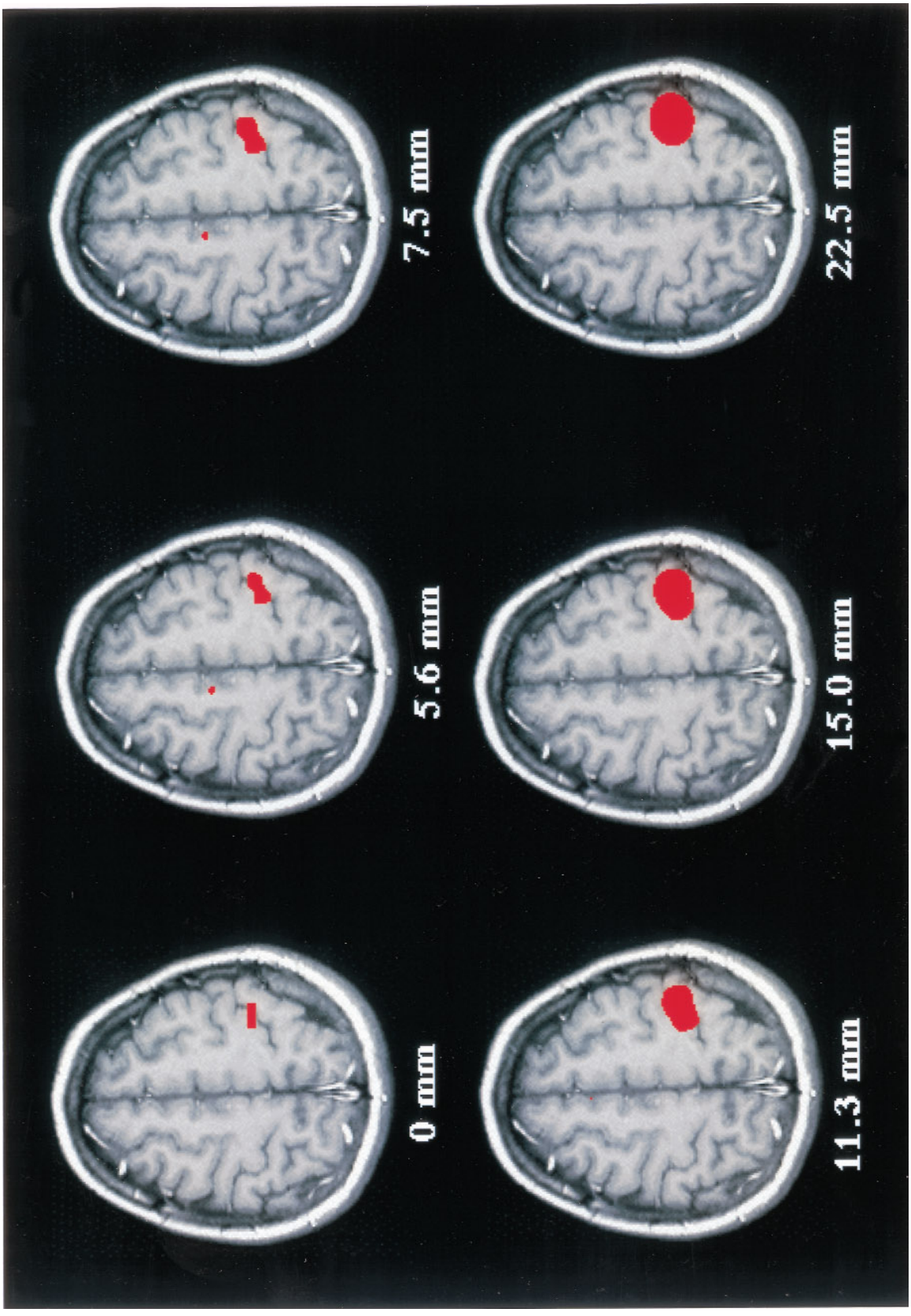

FIG. 3. The effect of spatial convolution on the extent of activation in the cerebral blood flow difference image. Cerebral blood flow images were convolved with a Gaussian kernel having the FWHM (mm) given below each image. Regions marked in red had statistically significant differences in cerebral blood flow during finger tapping ($t_{crit} = 4.17$). Data from subject 3.

assumed to be $N_1 + N_2 - 2 = 93$. This assumption is true in the absence of temporal correlation between cerebral blood flow images. Temporal correlation between images was investigated by computing the autocorrelation functions for time series of cerebral blood flow values obtained at various fixed voxel locations. The observed serial correlation coefficients were tested for significance using the standard error expected under the assumption of a white-noise process of equal length (Box and Jenkins, 1970), but were not different from zero ($P > 0.05$) outside of the activated regions of the brain.

The threshold for statistical significance in the t images, t_{crit}, was calculated by correcting the image-based P value to obtain a voxel-based P value. The voxel-based P value was calculated using the Bonferroni correction, i.e., by dividing the image-based P value by the number of brain voxels in the original 64×64 image. The average number of brain voxels in the 64×64 images was 670 ± 77. When Gaussian convolution was applied the Bonferroni correction was too conservative, because spatial correlation reduced the number of independent resolution elements ("resels") (Worsley *et al.*, 1996a). No correction was applied to compensate for multiple tests using different Gaussian kernel widths (Worsley *et al.*, 1996b).

RESULTS

Cerebral blood flow values were calculated from the observed values of $\Delta M/M_0$, the fractional change in MR amplitude produced by arterial tagging, using Eq. [1] (see Materials and Methods).

Figure 2a shows an average cerebral blood flow image obtained during the combined finger-tapping period, while Fig. 2b shows the average cerebral blood flow image obtained from the same subject during the combined rest period. Figure 2c shows the cerebral blood flow difference image, i.e., the difference between cerebral blood flow images taken during finger-tapping and rest conditions, and Fig. 2d shows an image of the pooled standard deviation of the cerebral blood flow image. While images of the standard deviation of ΔM were spatially homogeneous (data not shown), images of the standard deviation of the calculated cerebral blood flow values were not homogeneous (see Fig. 2d), because of the spatial heterogeneity in R_{10} and $R_1(\omega_1, \Delta\omega)$ (see Eqs. [1]–[4]).

The cerebral blood flow difference image shown in Fig. 2c and the pooled standard deviation image shown in Fig. 2d were used to calculate a t score for each voxel, using Eq. [5]. A critical t value for statistically significant changes in cerebral blood flow during finger tapping, t_{crit}, was calculated using a P value of 0.05 for the slice and using a standard Bonferroni correction (see Materials and Methods). The average value of t_{crit} for the seven subjects was 4.14 ± 0.03.

Regions of the cerebral blood flow difference image having a t score larger than t_{crit} are shown in red in Fig. 3, superimposed on anatomical MRI. The areas of the activated regions depend on the width of the Gaussian kernel used to convolve the cerebral blood flow images. For example, increasing the width of the Gaussian kernel increased the area of the activated primary sensorimotor cortex region, but decreased the average change in cerebral blood flow (see Table 1). Similar results were observed for all subjects (see Table 2).

For the data shown in Fig. 3 activation was observed in the supplementary motor area for intermediate, but not for low or high, values of the Gaussian kernel width (see Table 1). Similar results were observed for five of the seven subjects (data not shown). Two subjects did not display statistically significant activation in the supplementary motor area for any of the Gaussian kernel widths.

Figure 4 shows cerebral blood flow "activation" maps for all seven subjects. The activation maps were obtained using a Gaussian kernel width of 5.6 mm. Under these conditions every subject showed a region of activated cerebral blood flow in the contralateral primary sensorimotor cortex. The mean area of the activated region in the contralateral primary sensorimotor cortex was 123 ± 34 mm^2, and the mean increase in cerebral blood flow in the activated region was 39 ± 6 cc/100 g/min ($63 \pm 22\%$). In addition, five subjects showed a region of activated cerebral blood flow in the supplementary motor area. The mean area of the activated region of the supplementary motor area in these five subjects was 13 ± 12 mm^2, and the mean increase in cerebral blood flow in the activated area was 31 ± 19 cc/100 g/min ($52 \pm 40\%$).

Figure 5 shows a plot of the average cerebral blood flow obtained for the activated primary sensorimotor cortex regions shown in Fig. 4, as a function of the average cerebral blood flow observed in the same region during rest. Figure 5 also shows a plot of the difference between the activated and the resting cerebral blood flow in the activated primary sensorimotor cortex region as a function of the resting cerebral blood flow in this region. The average increase in cerebral blood flow was 39 ± 6 cc/100 g/min. Linear regression analysis demonstrated that this increase in cerebral blood flow did not have a statistically significant dependence on the resting cerebral blood flow ($P = 0.05$).

DISCUSSION

Finger-tapping paradigms would be expected to increase cerebral blood flow in the contralateral primary

TABLE 1

Effect of Gaussian Convolution on the Area and Average Cerebral Blood Flow Increase, ΔCBF, of Activated Contralateral Primary Sensorimotor Cortex (PSMC) and Activated Supplementary Motor Area (SMA) Regions

Kernel width[a] (mm)	PSMC		SMA	
	Area[b] (mm^2)	ΔCBF[c] (cc/100 g/min)	Area[b] (mm^2)	ΔCBF[c] (cc/100 g/min)
0	42	72 (94%)[d]	—	—
5.6	89	47 (70%)	8	52 (113%)[d]
7.5	127	45 (70%)	9	48 (93%)
11.3	246	31 (52%)	—	—
15.0	318	27 (45%)	—	—
22.5	365	23 (37%)	—	—

Note. Data from subject 3 (see Fig. 3).

[a] FWHM of the Gaussian kernel used to convolve the cerebral blood flow images.

[b] Area of the region having a statistically significant increase in cerebral blood flow during the finger tapping task.

[c] Average cerebral blood flow increase in the activated area.

[d] Percentage increase in average cerebral blood flow.

sensorimotor cortex and the supplementary motor area (Roland *et al.*, 1980). The major aim of this work was to investigate if arterial spin tagging approaches could detect and quantitate these regional cerebral blood flow increases.

Figure 3 shows that the size of the activated area of the primary sensorimotor cortex, and the average increase in cerebral blood flow in this area, varied according to the width of the Gaussian kernel used to convolve the cerebral blood flow images. For example, if no convolution was applied, the size of the activated primary sensorimotor cortex region was 42 mm^2 and the average increase in cerebral blood flow was 72 cc/100 g/min (94%) (see Table 1). However, if the cerebral blood flow images were convolved with a Gaussian kernel width of 15 mm, the size of the activated primary sensorimotor cortex region was 318 mm^2 and the average increase in cerebral blood flow was 27 cc/100 g/min (45%). In the absence of spatial convolution the statistical analysis recognized a small area with a large average increase in cerebral blood flow, while in the presence of spatial convolution the statistical analysis recognized a large area with a small average increase in cerebral blood flow.

Figure 3 also shows that there appears to be an "optimum" Gaussian kernel width for observation of statistically significant increases in cerebral blood flow in the supplementary motor area with this technique. For example, for a Gaussian kernel of 5.6 or 7.5 mm statistically significant increases in cerebral blood flow are observed in the supplementary motor area. However, for Gaussian kernels smaller or larger than these values no statistically significant increases in cerebral blood flow were observed in this area. The optimum Gaussian kernel thus provides the maximum statistical power for observation of cerebral blood flow increases in the supplementary motor area. For a single, focal activation the optimum filter is approximately equal to the size of the activated area (Rosenfeld and Kak, 1982; Worsley, 1996b). If no information on the size of the activated area is available, wavelet approaches could be used to estimate the optimum kernel width (Ruttimann *et al.*, 1996).

Figure 4 shows that if the cerebral blood flow images are convolved with a 5.6-mm Gaussian kernel, statistically significant increases in cerebral blood flow are observed during the finger tapping task in the contralateral primary sensorimotor cortex of all subjects and in the supplementary motor area of most subjects. Under these conditions, the average increase in cerebral blood flow in the activated area of the primary sensorimotor cortex was 39 ± 6 cc/100 g/min and was not dependent on the resting cerebral blood flow value (see Fig. 5).

While statistically significant cerebral blood flow activation was observed in the primary sensorimotor cortex for all subjects, statistically significant activation was not observed in the supplementary motor area for all subjects (see Fig. 4). The intersubject variability observed in the position of the activated supplementary motor area (see Fig. 4) could be due to intrinsic individual variability (Mattay *et al.*, 1996), but could also be due to variability in the position of the imaging slice with respect to the location of the supplementary motor area. Extension of the arterial spin tagging

TABLE 2

Effect of Gaussian Convolution on the Area and Average Cerebral Blood Flow Increase of Activated Contralateral Primary Sensorimotor Cortex (PSMC): Mean Results from Seven Subjects

Kernel width[a] (mm)	⟨Area⟩[b] (mm^2)	⟨ΔCBF⟩[c] (cc/100 g/min)
0	41 ± 12	60 ± 10 (91 ± 32%)[d]
5.6	123 ± 34	39 ± 6 (63 ± 22%)
7.5	181 ± 68	35 ± 7 (57 ± 20%)
11.3	298 ± 99	27 ± 6 (46 ± 16%)
15.0	395 ± 137	23 ± 7 (42 ± 15%)
22.5	438 ± 221	24 ± 11 (42 ± 19%)

[a] FWHM of the Gaussian kernel used to convolve the cerebral blood flow image.

[b] Mean (±SD) area of the primary sensorimotor cortex region having a statistically significant increase in cerebral blood flow during the finger tapping paradigm.

[c] Mean (±SD) of average increase in cerebral blood flow in the activated primary sensorimotor cortex area during the finger tapping task.

[d] Percentage increase in average cerebral blood flow.

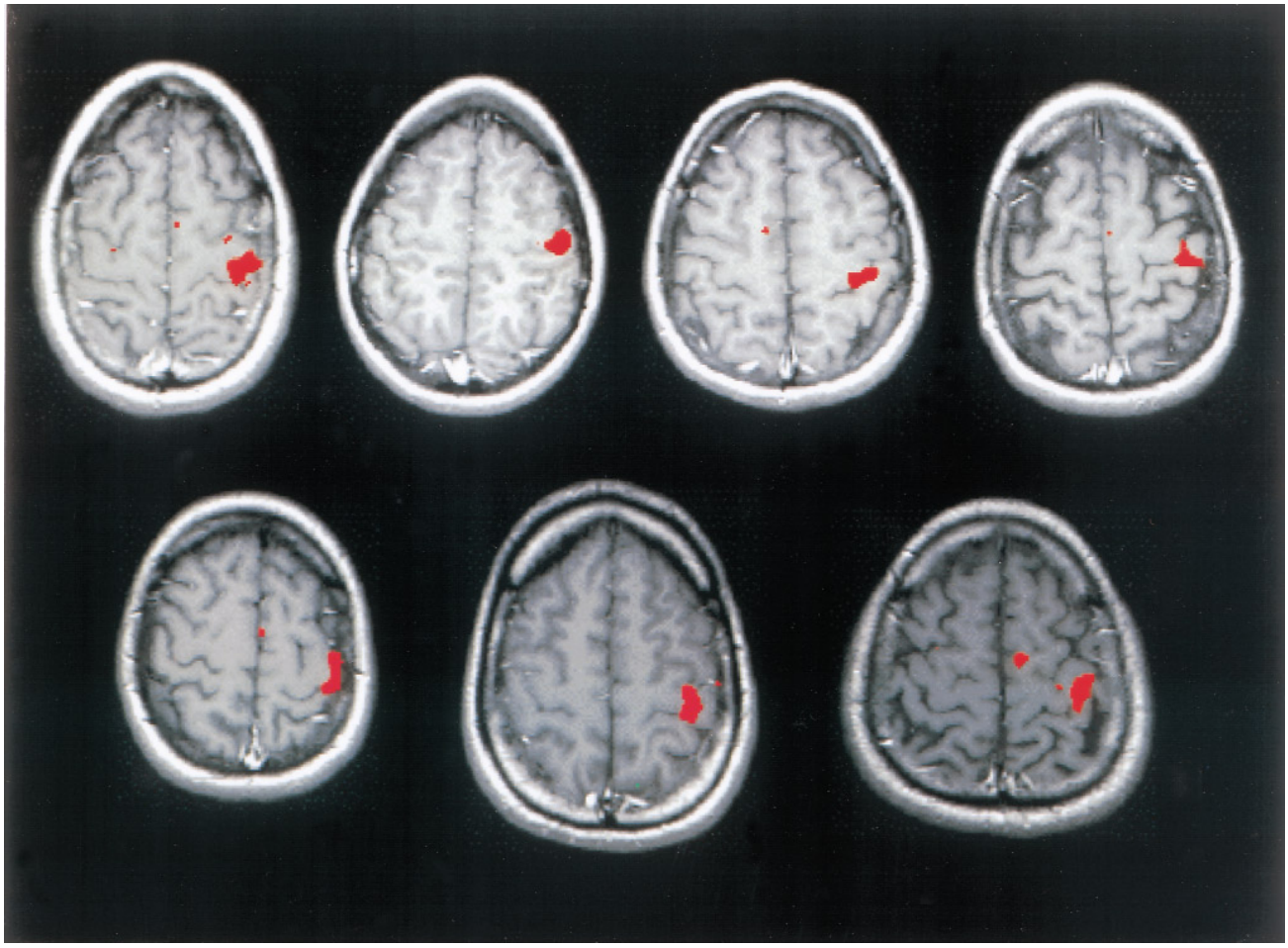

FIG. 4. Cerebral blood flow activation images for seven control subjects. Cerebral blood flow images were convolved with a Gaussian kernel having a FWHM of 5.6 mm. Regions marked in red had statistically significant differences in cerebral blood flow during finger tapping.

approach to provide three-dimensional cerebral blood flow images would alleviate this problem.

Cerebral blood flow increases observed using steady-state arterial spin tagging techniques can be compared with cerebral blood flow increases observed using other approaches. ^{133}Xe (Roland *et al.*, 1980), $^{11}CH_3F$ PET (Sietz and Roland, 1992), and H_2 ^{15}O PET (Colebatch *et al.*, 1991; Ramsey *et al.*, 1996) studies have reported cerebral blood flow increases of approximately 25–40% in the primary sensorimotor cortex during finger tapping. Assuming that the effective width of the point-spread function for these approaches was 10–20 mm, the cerebral blood flow increases observed using arterial spin tagging approaches are comparable to those observed using ^{133}Xe and PET (see Table 2).

The results discussed above explain why techniques that have different intrinsic spatial resolution can give apparently different increases in cerebral blood flow during motor activation. From the data presented here we conclude that regional cerebral blood flow in the primary sensorimotor cortex increased by at least 91% during motor activation (see Table 2). However, if cerebral blood flow changes were confined to a region that was smaller than the intrinsic spatial resolution of the spin tagging approach, the actual focal increase in cerebral blood flow could be larger than 91%.

The MR techniques used in the present study are slightly different from those used in our previous steady-state arterial spin tagging studies (Ye *et al.*, 1997a). First, we used SPIRAL rather than EPI, because the shorter TE increased the signal-to-noise ratio of the cerebral blood flow images. Second, we used "delayed acquisition" arterial spin tagging approaches (Alsop and Detre, 1996; Ye *et al.*, 1997c), because the time required for the measurements was decreased and the sensitivity to variation in the arterial transit time was minimized. Recent studies have shown that cerebral blood flow values calculated using delayed acquisition spin tagging approaches agree well with cerebral blood flow values determined in the same slice, and in the same subject, using ^{15}O PET approaches (Ye *et al.*, 1997b).

In summary, steady-state arterial spin tagging ap-

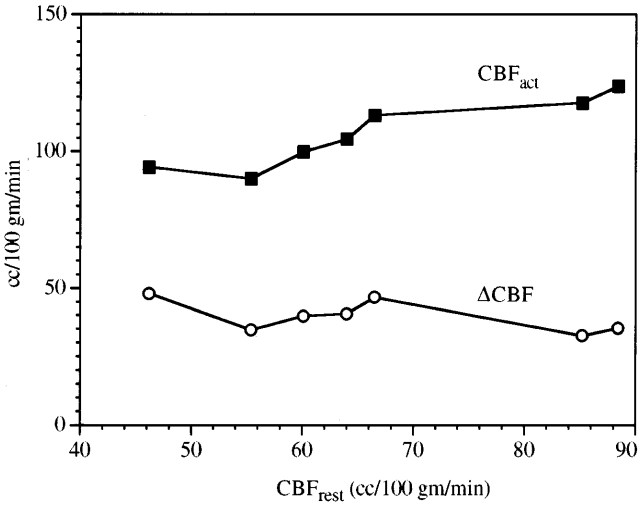

FIG. 5. (Filled symbols) Plot of the average cerebral blood flow in activated contralateral primary sensorimotor cortex regions during finger tapping, CBF_{act}, against the average cerebral blood flow in the same region during rest, CBF_{rest}. Each point arises from a different subject. (Open symbols) Plot of the increase in cerebral blood flow in activated contralateral primary sensorimotor cortex regions, ΔCBF, against CBF_{rest}. Cerebral blood flow images were convolved with a Gaussian filter having a FWHM of 5.6 mm (see Fig. 4).

proaches can provide quantitative images of statistically significant regional increases in cerebral blood flow during motor activation paradigms.

ACKNOWLEDGMENTS

We are grateful for many helpful discussions with Jack Leigh and the staff of the MMRRCC at the University of Pennsylvania.

REFERENCES

Alsop, D. C., and Detre, J. A. 1996. Reduced transit-time sensitivity in noninvasive magnetic resonance imaging of human cerebral blood flow. *J. Cereb. Blood Flow Metab.* **16:** 1236–1249.

Bandettini, P. A., Wong, E. C., Hinks, R. S., Tikofsky, R. S., and Hyde, J. S. 1992. Time course of EPI of human brain function during task activation. *Magn. Reson. Med.* **25:**390– 397.

Box, G. E. P., and Jenkins, G. M. 1970. *Time Series Analysis for Forecasting and Control,* pp. 34–36. Holden-Day, San Francisco.

Colebatch, J. G., Deiber, M.-P., Passingham, R. E., Friston, K. J., and Frackowiak, R. S. J. 1991. Regional cerebral blood flow during voluntary arm and hand movements in human subjects. *J. Neurophysiol.* **65:**1392–1401.

Detre, J. A., Leigh, J. S., Williams, D. S., and Koretsky, A. P. 1992. Perfusion imaging. *Magn. Reson. Med.* **23:**37–45.

Edelman, R. R., Siewert, B., Darby, D. G., Thangaraj, V., Nobre, A. C., Mesulam, M. M., and Warach, S. 1994. Quantitative mapping of cerebral blood flow and functional localization with echo-planar MR imaging and signal targeting with alternating radio frequency. *Radiology* **192:**513–520.

Kim, S-G. 1995. Quantification of relative cerebral blood flow change by flow-sensitive alternating inversion recovery (FAIR) technique: Application to functional mapping. *Magn. Reson. Med.* **34:**293–301.

Kim, S-G., and Tsekos, N. V. 1997. Perfusion imaging by a flow-sensitive alternating inversion recovery (FAIR) technique: Application to functional brain imaging. *Magn. Reson. Med.* **37:**425–435.

Kwong, K. K., Belliveau, J. W., Chesler, D. A., Golberg, I. E., Weisskoff, R. M., Poncelet, B. P., Kennedy, D. N., Hopper, B. E., Cohen, M. S., Turner, R., Cheng, H.-M., Brady, T. J., and Rosen, B. R. 1992. Dynamic magnetic resonance imaging of human brain activity during primary sensory stimulation. *Proc. Natl. Acad. Sci. USA* **89:**5675– 5679.

Kwong, K., Chesler, D. A., Weisskoff, R. M., Donahue, K. M., Davis, T. L., Ostergaard, L., Campbell, T. A., and Rosen, B. R. 1995. MR perfusion studies with T1-weighted echo planar imaging. *Magn. Reson. Med.* **34:**878–887.

Mattay, V. S., Frank, J. A., Santha, A. K. S., Pekar, J. J., Duyn, J. H., McLaughlin, A. C., and Weinberger, D. R. 1996. Whole brain functional mapping with isotropic MR imaging. *Radiology* **201:**399–404.

Ogawa, S., Tank, D. W., Menon, R., Ellermann, M., Kim, S. G., Mekle, H., and Ugurbil, K. 1992. Intrinsic signal changes accompanying sensory stimulation: Functional brain mapping with magnetic resonance imaging. *Proc. Natl. Acad. Sci. USA* **89:**5951– 5955.

Ott, L. 1977. *An Introduction to Statistical Methods and Data Analysis,* pp. 113–115. Duxbury, Boston.

Pekar, J., Jezzard, P., Roberts, D. A., Leigh, J. S., Frank, J. A., and McLaughlin, A. C. 1996. Perfusion imaging with compensation for asymmetric magnetization transfer effects. *Magn. Reson. Med.* **35:** 70–79.

Ramsey, N. F., Kirkby, B. S., van Gelderen, P., Berman, K. F., Duyn, J. H., Frank, J. A., Mattay, V. S., van Horn, J. D., Esposito, G., Moonen, C. T. W., and Weinberger, D. R. 1996. Functional mapping of human sensorimotor cortex with 3D BOLD fMRI correlates highly with $H_2{}^{15}O$ PET rCBF. *J. Cereb. Blood Flow Metab.* **16:**755–764.

Roberts, D. A., Detre, J. A., Bolinger, L., Insko, E. K., and Leigh, J. S. 1994. Quantitative magnetic resonance imaging of human brain perfusion at 1.5 T using steady-state inversion of arterial water. *Proc. Natl. Acad. Sci. USA* **91:**33–37.

Roland, P. E., Larsen, B., Lassen, N. A., and Skinhoj, E. 1980. Supplementary motor area and other cortical areas in organization of voluntary movements in man. *J. Neurophysiol.* **43:**118–136.

Rosenfeld, A., and Kak, A. C. 1982. *Digital Picture Processing,* Vol. 2. Academic Press, Orlando, FL.

Ruttimann, U. E., Unser, M., Thévenaz, P., Lee, C., Rio, D., and Hommer, D. W. 1996. Statistical analysis of image differences by wavelet decomposition. In *Wavelets in Medicine and Biology* (A. Aldroubi and M. Unser, Eds.), pp. 115–144. CRC Press, Boca Raton, FL.

Seitz, R. J., and Roland, P. E. 1992. Learning of sequential finger movements in man: A combined kinematic and positron emission tomography (PET) study. *Eur. J. Neurosci.* **4:**154–165.

Talagala, S. L., Noll, D. C., and Thulborn, K. R. 1996. Functional MRI using steady-state arterial water labeling. *Abstr. Int. Soc. Magn. Reson. Med.* **4:**340.

Williams, D. S., Detre, J. A., Leigh, J. S., and Koretsky, A. P. 1992. Magnetic resonance imaging of perfusion using spin inversion of arterial water. *Proc. Natl. Acad. Sci. USA* **89:**212–216.

Worsley, K. J., Marrett, S., Neelin, P., Vandal, A. C., Friston, K. J., and Evans, A. C. 1996a. A unified statistical approach for determining significant signals in images of cerebral activation. *Hum. Brain Mapping* **4:** 58–73.

Worsley, K. J., Marrett, S., Neelin, P., and Evans, A. C. 1996b. Searching scale space for activation in PET images. *Hum. Brain Mapping* **4:**74–90.

Yang, Y., Glover, G. H., van Gelderen, P., Mattay, V. S., Santha, A. K. S., Sexton, R., Ramsey, N. F., Moonen, C. T. W., Weinberger, D. R., Frank, J. A., and Duyn, J. 1996. Fast 3D functional magnetic resonance imaging at 1.5T with spiral acquisition. *Magn. Reson. Med.* **36:** 620–626.

Ye, F. Q., Pekar, J. J., Jezzard, P., Duyn, J., Frank, J. A., and McLaughlin, A. C. 1996. Perfusion imaging of the human brain at 1.5 T using a single-shot EPI spin tagging approach. *Magn. Reson. Med.* **36:**219–224.

Ye, F. Q., Mattay, V. S., Jezzard, P., Frank, J. A., Weinberger, D. R., and McLaughlin, A. C. 1997a. Correction for vascular artifacts in cerebral blood flow values measured using arterial spin tagging techniques. *Magn. Reson. Med.* **37:** 226–235.

Ye, F. Q., Berman, K. F., Ellmore, T., Esposito, G., van Horn, J. D., Yang, Y., Duyn, J., Salustri, C., Smith, A. M., Frank, J. A., Weinberger, D. R., and McLaughlin, A. C. 1997b. H_2 ^{15}O PET validation of arterial spin tagging measurements of cerebral blood flow in humans. *Abstr. Int. Soc. Magn. Reson. Med.* **5:** 87.

Ye, F. Q., Mattay, V. S., Frank, J. A., Weinberger, D. R., and McLaughlin, A. C. 1997c. Calculation of cerebral blood flow using "delayed acquisition" arterial spin tagging approaches. *Abstr. Int. Soc. Magn. Reson. Med.* **5:**1756.